Theory of inhomogeneous quantum systems. I. Static properties of Bose fluids

E. Krotscheck,* G.-X. Qian, and W. Kohn
Institute for Theoretical Physics, University of California, Santa Barbara, California 93106
(Received 30 March 1984)

We develop a variational theory for the determination of the ground-state properties of an inhomogeneous Bose fluid at zero temperature. Euler-Lagrange equations are derived for the one- and two-body correlations, and systematic approximation methods are physically motivated. It is shown that the optimized variational method provides a self-consistent approximate summation of ladder and ring diagrams. Numerical applications are presented for the density profile, distribution functions, energy, and chemical potential of films of ^{4}He atoms. Both the bulk and surface energies are calculated and found to be in fair agreement with experiments.

I. INTRODUCTION

Based on the success of variational methods within the last decade we may regard the ground state of simple quantum liquids such as the helium isotopes and the electron gas as well understood. Doubtless, the solution of the many-body Schrödinger equation for these systems[1-3] by means of the Green's-function Monte Carlo (GFMC) method at present provides the best answer for the ground state of these systems. Nevertheless, many-body methods based on variational (Jastrow-type) wave functions,[4] cluster expansions, resummation techniques, and an optimization procedure also belong to the indispensable repertoire of modern microscopic many-body theory. Encouraged by the qualitative successes of these methods in the theory of bulk quantum liquids, we seek an extension to the more complicated case of inhomogeneous systems. This paper is the first in a series of papers in which we address ourselves to the theoretical formulation and numerical application of the variational theory of inhomogeneous systems. As the simplest species of physical interest, we will present here the application of the theory to the static properties of films of ^{4}He atoms. This work is done not only because of the interest in this physical system, but also as a first step to explore the possibilities of an extension of variational theories for the surface of Fermi systems, in particular the electron gas in a metal surface.

A few points are worth mentioning to relate the variational approach to both conventional, perturbative many-body theory and Monte Carlo methods, and to provide motivation for some of the further developments of this paper.

(i) A satisfactory theory for a quantum system should be able to decide whether at zero temperature a given number A of interacting particles within a certain volume V is in a homogeneous or in an inhomogeneous state. If the particle number if large enough (to be specific we think of a system of ^{4}He atoms) the volume will be filled with a homogeneous liquid of positive pressure. As we decrease the particle number we will first enter a metastable regime with negative pressure, and finally encounter a local instability due to a vanishing compressibility. Such a physical instability should also be reflected in a corresponding instability of the theoretical description of the system. This physically rather natural requirement is satisfied by the variational theory using hypernetted-chain (HNC) methods[4] and by the parquet-diagram theory.[5]

(ii) Variational/integral-equation methods (to be specific, we refer here again to the HNC integral equations for the summation of infinite series of cluster diagrams) contain the two most prominent methods of conventional many-body theory, the sum of the ring and ladder diagrams, as simple special cases.[5]

(iii) Variational/integral-equation theories for *homogeneous* systems require very small computational effort. They reflect the known physical instabilities of a quantum liquid, at low densities against the above-mentioned formation of droplets, and at high densities against solidification.[6]

(iv) Monte Carlo simulations usually start from a variational wave function of (generalized) Jastrow form, and converge more quickly the more realistic the starting functions are. A good choice of a starting function is usually quite easy in a bulk quantum liquid, but requires more thought in an inhomogeneous system.

(v) Variational methods can be extended in a straightforward way to a theory of the low-lying excited states of a quantum liquid. This theory is collectively known as correlated-basis-functions theory[4] and emerges today essentially as a theory of effective interactions between quasiparticles to be used in precisely those places, where conventional (perturbative) many-body approaches become entangled in insurmountable technical problems.[7]

A few attempts have been made to derive a variational theory of the surface of liquid ^{4}He. Most notable is the early work of Woo and collaborators,[8] a similar study by Chang and Cohen,[9] and a somewhat more recent work by Saarela *et al.*[10] Common to these papers is that the relevant two-body densities were considered to be isotropic, and that local-density approximations were made for these functions. Beyond this, Saarela *et al.*[10] have derived a set of equations that should in principle also give access to the study of anisotropies. These authors found, however, the fully self-consistent solutions of the hypernetted-chain equations in an inhomogeneous system, and the op-

 ©1985 The American Physical Society

timization of the Jastrow functions, to be numerically too difficult to execute. This difficulty is in contrast to the experience gained from variational theories for homogeneous quantum liquids, where HNC and optimization methods provide presently the best tradeoff between the accuracy of the prediction of physical quantities and the numerical effort involved.

Local-density approximations have their well-known problems in the low-density regime. But there is some indication that, for very small separations, the correlations in the surface of a quantum liquid are in fact isotropic. Of course, the phrase "very small separations" calls for specification, which will be given along with the further developments of our theory. On the other hand, there is little reason to assume that the correlations at intermediate and large separations (i.e., those of the order of the range of the surface thickness) are isotropic, though this anisotropy cannot be easily detected in the simplest ground-state properties such as the density distribution.[11] It is one of the purposes of this paper to explore these anisotropies. In this sense, our work goes beyond comparable earlier studies.

Our work provides the first successful fully consistent application of variational and integral-equation methods to an inhomogeneous system. It is characterized by the advantages of optimization procedures and the systematics of integral-equation theories known from studies of bulk quantum liquids.[6] We concentrate here on the simplest acceptable[12] implementation of integral-equation methods, which is collectively known as the hypernetted-chain approximation.[13,14]

For some of the bulk properties of inhomogeneous systems it is possible to perform variational and Green's-function Monte Carlo calculations.[11] Our theory is to be understood as being complementary, not in competition with Monte Carlo methods. It is clear that the inclusion of three-body factors and the automatic calculation of "elementary" diagrams in a variational Monte Carlo calculation will give, especially for high-density systems, more accurate estimates for gross properties. The HNC approximation in particular yields a too low value for the saturation density, and, of course, our calculation cannot improve this.

To what extent this drawback of the HNC is serious in considerations that go beyond the ground state remains to be seen. Generally, it is for the study of excited states more important to have a carefully optimized ground-state wave function than it is to have a slightly better estimate for the ground-state energy. The study of excited states on the background of a nonoptimized ground state will inevitably give rise to spurious instabilities simply reflecting the fact that the energy expectation value can be lowered by a better wave function. To give another example: The optimization of the pair correlations in bulk ^{4}He yields only a small amount of additional binding energy. Nevertheless, the optimization affects the long-wavelength part of the static form factor, and hence the phonon spectrum, quite notably. This correction is comparable to, and in most cases larger, than the effect of elementary diagrams and three-body correlations. We note also that the hypernetted-chain approximation becomes increasingly better as we approach the low-density regions of the surface.

The above reservations about the general usefulness of variational Monte Carlo calculations for problems which go beyond static properties do not, of course, apply to the GFMC aspect of Ref. 11. But it is questionable whether the GFMC theory can be extended to excited states,[15] and one must also keep in mind that the computational effort of the theory presented here is several orders of magnitude smaller than the one of a GFMC calculation. Of course, one may still legitimately question the usefulness of an HNC/EL (HNC/Euler-Lagrange) theory for surface problems if such a theory is restricted to the static properties already known from GFMC calculations or accessible by these techniques. We emphasized, therefore, from the outset the possibility to study excited states as well.

Another important point is worth mentioning: With GFMC data for the static properties (e.g., the static form factor) available one may work "backwards" through the equations of the variational theory, obtain a particle-hole interaction, and from that the dispersion relation for the collective modes. This program has recently successfully been carried through for the electron gas.[16]

The variational theory of anisotropic ^{4}He is doubtlessly numerically quite complicated compared with the theory of bulk ^{4}He. This complication is simply due to the amount of data to be handled. To represent a quantity like the two-body density in the homogeneous system requires about 50 to 100 data points. Due to the broken symmetry we need for the same quantity in the inhomogeneous case about 10^5 points. It is clear that the design of a numerical method to determine such large numbers of data requires some thought. A suitable strategy for solving the equations of the variational theory for an inhomogeneous system relies, therefore, even more on the understanding of the physical processes described by the formal quantities of the theory rather than in the bulk system. We will, therefore, emphasize the discussion of these points.

The main body of our paper consists of the formal development of the variational theory of inhomogeneous boson systems and the derivation of Euler-Lagrange equations for the optimization of the trial wave function. The basic quantities and equations will be introduced in Sec. II. Section III describes the optimization of the two-body correlations, and Sec. IV gives the corresponding manipulations for the one-body density. The proof that the ring diagrams of the conventional random-phase approximation (RPA) are a proper subset of the optimized HNC theory will be given in Sec. V.

Section VI is devoted to the description of the numerical optimization method used in our work. Section VII presents results on the static properties of films of ^{4}He. The final section, VIII, gives an overview of possible extensions of the present work to excited states and to Fermi systems.

The manipulations of this paper will occasionally be algebraically quite lengthy. This is caused by the fact that we are entering a rather unexplored field, reminiscent of the early developments of the variational theories of homogeneous systems.

II. VARIATIONAL WAVE FUNCTIONS, DISTRIBUTION FUNCTIONS, AND THE ENERGY EXPECTATION VALUE

A variational theory for a boson liquid starts with an *ansatz* for the many-body wave function of the Feenberg

$$\Psi_0(\mathbf{r}_1,\ldots,\mathbf{r}_A)=\exp\left[\frac{1}{2}\sum_{i=1}^{A}u_1(\mathbf{r}_i)+\frac{1}{2}\sum_{\substack{i<j\\ i,j=1}}^{A}u_2(\mathbf{r}_i,\mathbf{r}_j)+\frac{1}{2}\sum_{\substack{i<j<k\\ i,j,k=1}}^{A}u_3(\mathbf{r}_i,\mathbf{r}_j,\mathbf{r}_k)+\cdots\right]. \tag{2.1}$$

The decomposition of the Feenberg function into one-, two-, . . . , A-body correlations is made unique by requiring that each of the $u_i(\mathbf{r}_1,\ldots,\mathbf{r}_i)$, $i=1,2,\ldots,A$, satisfies the *cluster property,* i.e., it vanishes whenever one or more of the particles are sufficiently far away from the others. Here we will be concerned only with the one- and the two-body portions of the Feenberg function (2.1); most of the developments of the theory will be formally unaffected, though numerically complicated, by the possible presence of a three-body factor.

With the wave function (2.1) given, we introduce as usual the one- and two-body densities

$$\rho_1(\mathbf{r}_1)=A\frac{\int d^3r_2\cdots d^3r_A\,\Psi_0^2(\mathbf{r}_1,\ldots,\mathbf{r}_A)}{\int d^3r_1\cdots d^3r_A\,\Psi_0^2(\mathbf{r}_1,\ldots,\mathbf{r}_A)} \tag{2.2}$$

and

$$\rho_2(\mathbf{r}_1,\mathbf{r}_2)=A(A-1)\frac{\int d^3r_3\cdots d^3r_A\,\Psi_0^2(\mathbf{r}_1,\ldots,\mathbf{r}_A)}{\int d^3r_1\cdots d^3r_A\,\Psi_0^2(\mathbf{r}_1,\ldots,\mathbf{r}_A)}, \tag{2.3}$$

and the two-body distribution function

$$g(\mathbf{r}_1,\mathbf{r}_2)=\frac{\rho_2(\mathbf{r}_1,\mathbf{r}_2)}{\rho_1(\mathbf{r}_1)\rho_1(\mathbf{r}_2)}. \tag{2.4}$$

Provided that we neglect three-body correlations, the knowledge of the one- and two-body function $u_1(\mathbf{r})$, $\rho_1(\mathbf{r})$, $u_2(\mathbf{r}_1,\mathbf{r}_2)$, and $\rho_2(\mathbf{r}_1,\mathbf{r}_2)$ is sufficient for a calculation of the energy expectation value

$$H_{00}[\{u_i\}]=\frac{\int d^3r_1\cdots d^3r_A\,\Psi_0(\mathbf{r}_1,\ldots,\mathbf{r}_A)H\Psi_0(\mathbf{r}_1,\ldots,\mathbf{r}_A)}{\int d^3r_1\cdots d^3r_A\,\Psi_0^2(\mathbf{r}_1,\ldots,\mathbf{r}_A)} \tag{2.5}$$

of a system of identical particles in an external field $U_{\text{ext}}(\mathbf{r})$, interacting via the two-body interaction $v(|\mathbf{r}_i-\mathbf{r}_j|)$,

$$H=-\frac{\hbar^2}{2m}\sum_{i=1}^{A}\nabla_i^2+\sum_{i=1}^{A}U_{\text{ext}}(\mathbf{r}_i)+\sum_{\substack{i<j\\ i,j=1}}^{A}v(|\mathbf{r}_i-\mathbf{r}_j|). \tag{2.6}$$

The optimal strategy for the determination of the correlation factors $u_1(\mathbf{r}_1)$ and $u_2(\mathbf{r}_1,\mathbf{r}_2)$ is the *minimization* of the energy expectation value H_{00}, i.e., the solution of the Euler-Lagrange equations

$$\frac{\delta H_{00}[u_1,u_2]}{\delta u_1(\mathbf{r}_1)}=0 \tag{2.7}$$

and

$$\frac{\delta H_{00}[u_1,u_2]}{\delta u_2(\mathbf{r}_1,\mathbf{r}_2)}=0. \tag{2.8}$$

Of course, the program outlined above—the determination of the distribution functions from the variational *ansatz* (2.1) for the wave function and the solution of the Euler-Lagrange equations (2.7) and (2.8)—cannot be carried out exactly. Ultimately, we will have to resort to approximation schemes to relate the trial functions $u_1(\mathbf{r})$, $u_2(\mathbf{r}_1,\mathbf{r}_2)$ to the physical densities $\rho_1(\mathbf{r})$ and $\rho_2(\mathbf{r}_1,\mathbf{r}_2)$ in order to cast the problem in a numerically tractable form. As experience with the optimization in bulk ^{4}He has taught us,[12] care has to be exercised in the choice of approximation methods to relate the distribution functions to the wave function. Similar care is necessary in the treatment of the kinetic energy operator in order to maintain the boundedness of the *approximate* energy expectation value.

We can, of course, take advantage of the experience gained in the past for the bulk system. Following the same formal route,[12] we will avoid any premature approximations in order to maintain the exact structure of the equations until the point of numerical application is reached. In this sense, the present study is the generalization of earlier work[12] to inhomogeneous systems.

After these preliminary remarks let us now turn to the formulation of the problem in a form which lends itself to the manipulations necessary to formulate the Euler-Lagrange equations (2.7) and (2.8) for the one- and two-body functions $u_1(\mathbf{r})$ and $u_2(\mathbf{r}_1,\mathbf{r}_2)$. Once unique relations between these one- and two-body correlations and the corresponding distribution functions are given, we could regard $\rho_1(\mathbf{r})$ and/or $\rho_2(\mathbf{r}_1,\mathbf{r}_2)$ as the independent variables. In fact, it will turn out that $u_1(\mathbf{r}_1)$ can be totally eliminated in favor of $\rho_1(\mathbf{r}_1)$. The same elimination of $u_2(\mathbf{r}_1,\mathbf{r}_2)$ in favor of $\rho_2(\mathbf{r}_1,\mathbf{r}_2)$ is also possible,[10] but is of no technical advantage.

We have chosen in this work to use the Born-Green-Yvon (BGY) equation for the one-body function and the hypernetted-chain equation for the two-body functions to relate the wave function to the physical distribution functions (2.2) and (2.3). The BGY equation has, compared with an HNC theory for one-body density,[13] the advan-

tage of being exact for a given two-body distribution function:

$$\nabla_1 u_1(\mathbf{r}_1)=\frac{\nabla_1\rho_1(\mathbf{r}_1)}{\rho_1(\mathbf{r}_1)}-\int d^3r_2\,\rho_1(\mathbf{r}_2)g(\mathbf{r}_1,\mathbf{r}_2)\nabla_1 u_2(\mathbf{r}_1,\mathbf{r}_2)\ . \tag{2.9}$$

We use Eq. (2.9) to eliminate the explicit appearance of the one-body correlation factor $u_1(\mathbf{r})$ in the energy expectation value and consider instead $\rho_1(\mathbf{r})$ as the independent one-body function. This elimination is an important step[10] in the development of an optimization procedure: In general, one cannot guarantee that the solution of the two-body Euler-Lagrange equation (2.8) satisfies the "cluster property" $u_2(\mathbf{r}_1,\mathbf{r}_2)\to 0$ for $|\mathbf{r}_1-\mathbf{r}_2|\to\infty$ for *any* given $u_1(\mathbf{r})$. We will see, however, that the solutions of the two-body Euler-Lagrange equation are well behaved for *any* given one-body density of $\rho_1(\mathbf{r})$.

The HNC equations are derived by diagrammatical studies of the two-body distribution function, originally performed in classical imperfect gases.[14] They relate the two-body correlation factor $u_2(\mathbf{r}_1,\mathbf{r}_2)$ and the two-body distribution function $g(\mathbf{r}_1,\mathbf{r}_2)$ through auxiliary quantities $N(\mathbf{r}_1,\mathbf{r}_2)$, $X(\mathbf{r}_1,\mathbf{r}_2)$, and $E(\mathbf{r}_1,\mathbf{r}_2)$ representing sets of nodal (N), non-nodal (X), and elementary (E) diagrams:

$$g(\mathbf{r}_1,\mathbf{r}_2)=\exp[u_2(\mathbf{r}_1,\mathbf{r}_2)+N(\mathbf{r}_1,\mathbf{r}_2)+E(\mathbf{r}_1,\mathbf{r}_2)] \tag{2.10}$$

and the chain equation

$$N(\mathbf{r}_1,\mathbf{r}_2)=\int d^3r_3\,\rho_1(\mathbf{r}_3)[g(\mathbf{r}_1,\mathbf{r}_3)-1]X(\mathbf{r}_3,\mathbf{r}_2)\ , \tag{2.11}$$

where

$$X(\mathbf{r}_1,\mathbf{r}_2)\equiv g(\mathbf{r}_1,\mathbf{r}_2)-1-N(\mathbf{r}_1,\mathbf{r}_2)\ . \tag{2.12}$$

The function $E(\mathbf{r}_1,\mathbf{r}_2)$ can be represented diagrammatically by an infinite series of elementary diagrams which can be expressed as multidimensional integrals involving $\rho_1(\mathbf{r})$ and $g(\mathbf{r}_1,\mathbf{r}_2)$. [The level of HNC approximation is defined by the choice of $E(\mathbf{r}_1,\mathbf{r}_2)$; for example HNC/0 neglects the elementary diagrams altogether.]

The HNC equations provide a prescription for calculating the pair-distribution function from a given two-body correlation function $u_2(\mathbf{r}_1,\mathbf{r}_2)$ in precisely the same way in which the diagrammatic derivation of the HNC equation is done. Starting from an initial guess $N(\mathbf{r}_1,\mathbf{r}_2)=E(\mathbf{r}_1,\mathbf{r}_2)=0$, Eq. (2.10) yields a first approximation for $g(\mathbf{r}_1,\mathbf{r}_2)$. With this $g(\mathbf{r}_1,\mathbf{r}_2)$, a new guess for $N(\mathbf{r}_1,\mathbf{r}_2)$ [Eq. (2.11)] is calculated. In addition, the elementary diagrams must be calculated according to the level of HNC approximation in which one chooses to work. With these new estimates for $N(\mathbf{r}_1,\mathbf{r}_2)$ and $E(\mathbf{r}_1,\mathbf{r}_2)$, the pair-distribution function $g(\mathbf{r}_1,\mathbf{r}_2)$ is updated via Eq. (2.10), and the procedure is repeated until convergence is reached. Equivalently, one may use the HNC equations to calculate the pair-correlation function $u_2(\mathbf{r}_1,\mathbf{r}_2)$ from a given pair-distribution function $g(\mathbf{r}_1,\mathbf{r}_2)$.

It will occasionally be convenient to write convolution integrals of the kind introduced in Eq. (2.11) in the abbreviated form

$$[A*B](\mathbf{r}_1,\mathbf{r}_2)\equiv\int d^3r_3\,\rho_1(\mathbf{r}_3)A(\mathbf{r}_1,\mathbf{r}_3)B(\mathbf{r}_3,\mathbf{r}_2)\ . \tag{2.13}$$

We are now ready to formulate the energy-expectation value (2.5) with respect to a trial wave function of the form (2.1) with $u_3=u_4=\cdots=u_A=0$. As usual, the expectation value of the kinetic energy operator is transformed using the Jackson-Feenberg (JF) identity

$$\int d^3r_1\cdots d^3r_A\,\Psi_0\nabla_i^2\Psi_0=\tfrac{1}{2}\int d^3r_1\cdots d^3r_A\,\Psi_0^2\nabla_i^2\ln\Psi_0\ , \tag{2.14}$$

and may hence be expressed in terms of the one- and the two-body densities alone:

$$\langle T\rangle=-\int d^3r_1\,\rho_1(\mathbf{r}_1)\frac{\hbar^2}{8m}\nabla_1^2 u_1(\mathbf{r}_1)$$
$$-\tfrac{1}{2}\int d^3r_1\,d^3r_2\,\rho_2(\mathbf{r}_1,\mathbf{r}_2)\frac{\hbar^2}{8m}(\nabla_1^2+\nabla_2^2)u_2(\mathbf{r}_1,\mathbf{r}_2)\ . \tag{2.15}$$

Finally, using the BGY equation (2.9), we eliminate the one-body factor $u_1(\mathbf{r})$ in favor of the physical one-body density, and represent the total-energy expectation value in a form which will be the starting point for our further manipulations:

$$E=\int d^3r_1\,\rho_1(\mathbf{r}_1)\left[U_{\rm ext}(\mathbf{r}_1)+\frac{\hbar^2}{8m}|\nabla_1\ln\rho(\mathbf{r}_1)|^2\right]$$
$$+\tfrac{1}{2}\int d^3r_1\,d^3r_2\,\rho_1(\mathbf{r}_1)\rho_1(\mathbf{r}_2)g(\mathbf{r}_1,\mathbf{r}_2)v_{\rm JF}(\mathbf{r}_1,\mathbf{r}_2)$$
$$=E_{(1)}+E_{(2)}\ . \tag{2.16}$$

Here, $v_{\rm JF}(\mathbf{r}_1,\mathbf{r}_2)$ is the generalized Jackson-Feenberg interaction

$$v_{\rm JF}(\mathbf{r}_1,\mathbf{r}_2)\equiv v(|\mathbf{r}_1-\mathbf{r}_2|)$$
$$-\frac{\hbar^2}{8m}\left[\frac{1}{\rho_1(\mathbf{r}_1)}\nabla_1\rho_1(\mathbf{r}_1)\cdot\nabla_1+\frac{1}{\rho_1(\mathbf{r}_2)}\nabla_2\rho_1(\mathbf{r}_2)\cdot\nabla_2\right]u_2(\mathbf{r}_1,\mathbf{r}_2)\ . \tag{2.17}$$

In the representation (2.16), the energy expectation value is to be understood to be a functional of the one-body density $\rho_1(\mathbf{r})$ and the two-body correlation factor $u_2(\mathbf{r}_1,\mathbf{r}_2)$. The pair distribution $g(\mathbf{r}_1,\mathbf{r}_2)$ is then known from the HNC equations (2.10) and (2.11). We could at this point use these equations[10] to eliminate also the two-body correlation function $u_2(\mathbf{r}_1,\mathbf{r}_2)$, and to formulate the theory entirely in terms of the (physically observable) one- and two-body distribution functions. However, this additional elimination calls for the neglect of the elementary diagrams at this early point and obscures somewhat the physical content of the theory. Since the elimination of the two-body correlation factor does not lead to a simplification of the further formal manipulations, we choose here to regard the one-body density $\rho_1(\mathbf{r})$ and the two-body correlation factor $u_2(\mathbf{r}_1,\mathbf{r}_2)$ as independent variables.

III. OPTIMIZATION OF THE TWO-BODY CORRELATIONS

The energy expression (2.16) allows for a straightforward derivation of a variety of representations of the Euler-Lagrange equation (2.8) to determine the pair-correlation function and the two-body distribution function. Ultimately, the representation of the Euler-Lagrange equation will depend on the optimization strategy adopted for its numerical solution, i.e., an iterative procedure to improve an initial guess for the two-body function until convergence is reached. In order to motivate the formal manipulations of this section, let us briefly review the available optimization algorithms for the two-body correlation function $u_2(\mathbf{r}_1,\mathbf{r}_2)$ and the related pair-distribution function $g(\mathbf{r}_1,\mathbf{r}_2)$ for bulk ^{4}He. In the bulk limit, all two-body functions depend only on the distance $r=|\mathbf{r}_1-\mathbf{r}_2|$ between two particles.

The historically first optimization route has been derived by Campbell and Feenberg[17] in their paired-phonon analysis (PPA). The PPA derives a set of equations for the static form factor

$$S(k)=1+\rho\int d^3r[g(r)-1]e^{i\mathbf{k}\cdot\mathbf{r}}\,, \tag{3.1}$$

and a self-consistent particle-hole interaction. The PPA equations are

$$S(k)=[1+(4m\rho/\hbar^2k^2)\tilde{V}_{p\text{-}h}(k)]^{-1/2} \tag{3.2}$$

with

$$V_{p\text{-}h}(r)=g(r)v(r)+(\hbar^2/m)\,|\,\nabla\sqrt{g(r)}\,|^2+[g(r)-1]w_I(r)\,. \tag{3.3}$$

(The three-dimensional Fourier transform is denoted by a tilde.) The "induced interaction"[18] $w_I(r)$ is, in the HNC approximation $E(r)=0$, most conveniently represented in Fourier space:

$$\tilde{w}_I(k)=-\frac{\hbar^2k^2}{4m\rho}[2S(k)+1][1-S^{-1}(k)]^2\,. \tag{3.4}$$

We recover in Eq. (3.2) the RPA expression for the static form factor. The HNC-EL theory supplements the RPA with a microscopic theory of the particle-hole interaction $V_{p\text{-}h}(r)$.

An alternative way to formulate the Euler-Lagrange equations has been used by Lantto and Siemens (LS),[18] who express the optimization condition in coordinate space. They arrive in the HNC approximation at

$$\left[-\frac{\hbar^2}{m}\nabla^2+v(r)+w_I(r)\right]\sqrt{g(r)}=0\,. \tag{3.5}$$

The PPA and the LS formulations of the Euler-Lagrange equation are algebraically equivalent. They merely suggest different iteration paths for the determination of the $g(r)$ and $u_2(r)$. The distinctive difference between the two formulations of the Euler-Lagrange equations is that the PPA formulation allows for an iterative solution in the sense that one may, starting from a given guess for $g(r)$, calculate a particle-hole interaction $V_{p\text{-}h}(r)$ and improve upon the initial guess via Eq. (3.2) until convergence is reached. One iteration of the PPA equations is hardly more time consuming than one iteration of the HNC equations for a given, fixed pair-correlation function $u_2(r)$. However, the procedure converges slowly if one starts with a poor guess for the short-ranged part of the pair-correlation function.

In contrast to the PPA, the LS formulation of (3.4) of the Euler-Lagrange equation does not allow for an iterative solution in the sense that one may solve Eq. (3.5) for a given induced interaction $w_I(r)$ and then improve upon $w_I(r)$, using Eq. (3.4). Rather, one must linearize the equation[19] and employ a Newton-Raphson procedure. If this is done, the iterations usually converge rather fast, especially for the short-ranged part of $g(r)$.

It is clear that the linearization of the Euler-Lagrange equation in the sense of Lantto and Siemens leads to a forbidding numerical effort in inhomogeneous systems. We are therefore naturally led to a generalization of the paired-phonon analysis as a suggestive iterative procedure for the solution of the Euler-Lagrange equations, and the remainder of this section will be devoted to the algebraic manipulations leading to the generalization of Eq. (3.2) to inhomogeneous systems.

Some qualitative physical considerations give additional support to the generalization of the PPA as the most promising route by which a numerical solution of the Euler-Lagrange equations can be found. The inhomogeneity of the system should mostly affect the intermediate- and long-ranged correlations. The PPA is especially efficient in precisely that regime, whereas one has usually very good *a priori* estimates of the structure of the short-ranged correlations. In fact, we expect that for the otherwise more complicated problem of the electrons in a metal surface, the "RPA approximation," in which the particle-hole interaction is replaced by the bare two-body potential, may be sufficient for a semiquanitative description of anisotropic correlations.

Let us now turn to the algebraic manipulations necessary to derive the generalization of Eqs. (3.2) and (3.3) to inhomogeneous systems. The remainder of this section is of purely algebraic nature, and the reader who is less interested in these technical details may proceed immediately to Sec. IV. The final form of our two-body Euler-Lagrange equation will be repeated in Sec. VI.

The variational derivative (2.8) of the energy expectation value (2.16) consists of two structurally different pieces: (i) the variation with respect to the *explicit* appearance of the pair-correlation function $u_2(\mathbf{r}_1,\mathbf{r}_2)$ through the Jackson-Feenberg interaction (2.17), and (ii) the variation with respect to the *implicit* appearance through the two-body density. Note that the one-body part of the energy (2.16) does not contribute to the Euler-Lagrange equation (2.8) due to our choice of the independent variables. The Euler-Lagrange equation (2.8) takes the form

$$\frac{\hbar^2}{8m}[D(1)+D(2)]g(\mathbf{r}_1,\mathbf{r}_2)=g'(\mathbf{r}_1,\mathbf{r}_2)\,, \tag{3.6}$$

where we have abbreviated the derivative

$$D(i)=\rho_1^{-1}(\mathbf{r}_i)\nabla_i\rho_1(\mathbf{r}_i)\cdot\nabla_i \tag{3.7}$$

and introduced the generalized distribution function,

$g'(\mathbf{r}_1,\mathbf{r}_2)$, through the definition

$$\rho_1(\mathbf{r}_1)\rho_2(\mathbf{r}_2)g'(\mathbf{r}_1,\mathbf{r}_2)\equiv\int d^3r_3\,d^3r_4 v_{\rm JF}(\mathbf{r}_3,\mathbf{r}_4)\frac{\delta\rho_2(\mathbf{r}_3,\mathbf{r}_4)}{\delta u_2(\mathbf{r}_1,\mathbf{r}_2)}\ . \tag{3.8}$$

This representation of $g'(\mathbf{r}_1,\mathbf{r}_2)$ is convenient since integral equations for $g'(\mathbf{r}_1,\mathbf{r}_2)$ may be derived from integral equations (e.g., HNC) for $g(\mathbf{r}_1,\mathbf{r}_2)$ by "graphical differentiation,"[4] for example, of the diagrams summed by the HNC equations (2.10) and (2.11):

$$g'(\mathbf{r}_1,\mathbf{r}_2)=g(\mathbf{r}_1,\mathbf{r}_2)[v_{\rm JF}(\mathbf{r}_1,\mathbf{r}_2)+N'(\mathbf{r}_1,\mathbf{r}_2)+E'(\mathbf{r}_1,\mathbf{r}_2)], \tag{3.9}$$

$$N'(\mathbf{r}_1,\mathbf{r}_2)=[g'*(g-N-1)](\mathbf{r}_1,\mathbf{r}_2)+[(g-1)*(g'-N')](\mathbf{r}_1,\mathbf{r}_2)\ . \tag{3.10}$$

The equations (3.9) and (3.10) are generally referred to as the HNC′ equations. Graphically, each of the "primed" functions $g'(\mathbf{r}_1,\mathbf{r}_2)$, $N'(\mathbf{r}_1,\mathbf{r}_2)$, $E'(\mathbf{r}_1,\mathbf{r}_2)$, and $X'(\mathbf{r}_1,\mathbf{r}_2)\equiv g'(\mathbf{r}_1,\mathbf{r}_2)-N'(\mathbf{r}_1,\mathbf{r}_2)$ may be constructed from the corresponding "unprimed" object by replacing, in turn, each correlation factor $h_2(\mathbf{r}_1,\mathbf{r}_2)\equiv\exp[u_2(\mathbf{r}_1,\mathbf{r}_2)]-1$ by a "screened" interaction $\exp[u_2(\mathbf{r}_1,\mathbf{r}_2)]v_{\rm JF}(\mathbf{r}_1,\mathbf{r}_2)$. Either by the stated diagrammatic analogy, or in a somewhat lengthy algebraic manipulation by repeatedly using the "chain equation" (2.11) one derives the connection

$$g'(\mathbf{r}_1,\mathbf{r}_2)=X'(\mathbf{r}_1,\mathbf{r}_2)+[(g-1)*X'](\mathbf{r}_1,\mathbf{r}_2)+[X'*(g-1)](\mathbf{r}_1,\mathbf{r}_2)+[(g-1)*X'*(g-1)](\mathbf{r}_1,\mathbf{r}_2)\ . \tag{3.11}$$

One may now reformulate the Euler-Lagrange equations (3.6) and (3.11) by repeated application of the chain equation (2.11) and eventually arrive at

$$\frac{\hbar^2}{4m}\{[D(1)+D(2)]X(\mathbf{r}_1,\mathbf{r}_2)-[X*DX](\mathbf{r}_1,\mathbf{r}_2)\}=V_{p\text{-}h}(\mathbf{r}_1,\mathbf{r}_2) \tag{3.12}$$

with

$$V_{p\text{-}h}(\mathbf{r}_1,\mathbf{r}_2)\equiv X'(\mathbf{r}_1,\mathbf{r}_2)+\frac{\hbar^2}{8m}[D(1)+D(2)]X(\mathbf{r}_1,\mathbf{r}_2)\ . \tag{3.13}$$

The appearance of the combination $[D(1)+D(2)]X(\mathbf{r}_1,\mathbf{r}_2)$ on *both* sides of Eq. (3.12) [cf. the definition (3.13) of the particle-hole interaction] might seem strange to the initiated reader. We hasten, therefore, to explain that the term $[D(1)+D(2)]X(\mathbf{r}_1,\mathbf{r}_2)$ *cancels* the longest-range contributions to $X'(\mathbf{r}_1,\mathbf{r}_2)$ due to correlations. To see this, we expand, for large particle distances, the exponential (2.10) and find [cf. Eq. (2.12)]

$$u_2(\mathbf{r}_1,\mathbf{r}_2)\approx X(\mathbf{r}_1,\mathbf{r}_2),\quad |\mathbf{r}_1-\mathbf{r}_2|\to\infty\ . \tag{3.14}$$

Hence, the longest-ranged portion of the kinetic energy term in the Jackson-Feenberg interaction (2.17) is canceled exactly against the $[D(1)+D(2)]X(\mathbf{r}_1,\mathbf{r}_2)$ term in the particle-hole interaction (3.13). More is known in the bulk system, where the particle-hole interaction behaves asymptotically as

$$V_{p\text{-}h}(r)=g(r)v(r)+O(r^{-8}),\quad r\to\infty\ . \tag{3.15}$$

A few more manipulations may be performed, within the HNC *approximation* $E(\mathbf{r}_1,\mathbf{r}_2)=0$, $E'(\mathbf{r}_1,\mathbf{r}_2)=0$, in order to represent the particle-hole interaction in a somewhat more closed form. The EL equation may be used to eliminate $X'(\mathbf{r}_1,\mathbf{r}_2)$ from the HNC′ equations (3.9) and (3.10) to yield

$$N'(\mathbf{r}_1,\mathbf{r}_2)=\frac{\hbar^2}{8m}\{[D(1)+D(2)]N(\mathbf{r}_1,\mathbf{r}_2)+2[X*DX](\mathbf{r}_1,\mathbf{r}_2)\}\ , \tag{3.16}$$

and eliminating $u_2(\mathbf{r}_1,\mathbf{r}_2)$ by use of the HNC equations leads to a useful form of the particle-hole interaction

$$V_{p\text{-}h}(\mathbf{r}_1,\mathbf{r}_2)=g(\mathbf{r}_1,\mathbf{r}_2)v(|\mathbf{r}_1-\mathbf{r}_2|)+\frac{\hbar^2}{2m}\{|\nabla_1[g(\mathbf{r}_1,\mathbf{r}_2)]^{1/2}|^2+|\nabla_2[g(\mathbf{r}_1,\mathbf{r}_2)]^{1/2}|^2\}+\frac{\hbar^2}{4m}[g(\mathbf{r}_1,\mathbf{r}_2)-1]\{[D(1)+D(2)]N(\mathbf{r}_1,\mathbf{r}_2)+[X*DX](\mathbf{r}_1,\mathbf{r}_2)\}\ . \tag{3.17}$$

With the representation (3.12) of the Euler-Lagrange equation we have derived the generalization of the PPA equations (3.2)—(3.4) for inhomogeneous systems (note that $S(k)=1/[1-\rho\tilde{X}(k)]$). These equations allow for an iterative numerical solution which will be described in detail in Sec. V. The form (3.17) of the particle-hole interaction is used mainly for numerical convenience. To understand the physical significance of the distinct diagrammatic quantities, it is easier to start from the form (3.13) of the particle-hole interaction.[12,20]

IV. ONE-BODY WAVE FUNCTIONS

We have so far considered the one-body density as a fixed function. The final step in our procedure to derive a closed set of equations for the one- and two-body distribution functions is to determine the one-body density $\rho_1(\mathbf{r})$ by minimization of the energy expectation value (2.16). To some extent, our derivations parallel those of Saarela *et al.*, but some reformulation of the theory is necessary in order to fit it into our emphasis of the PPA as the optimization procedure.

A convenient quantity to consider as the variable is $\sqrt{\rho_1(\mathbf{r})}$. The particle number is kept constant, i.e., we consider

$$\frac{\delta}{\delta\sqrt{\rho_1(\mathbf{r}_1)}}\left[\int d^3r_1\left[\rho_1(\mathbf{r}_1)[U_{\rm ext}(\mathbf{r}_1)-\mu]+\frac{\hbar^2}{2m}\,|\,\nabla\sqrt{\rho_1(\mathbf{r}_1)}\,|^2\right]+\tfrac{1}{2}\int d^3r_1 d^3r_2\,\rho_1(\mathbf{r}_1)\rho_1(\mathbf{r}_2)g(\mathbf{r}_1,\mathbf{r}_2)v_{\rm JF}(\mathbf{r}_1,\mathbf{r}_2)\right]=0\ . \tag{4.1}$$

We write (4.1) in a form reminiscent of the Hartree equation, i.e., as

$$0=-\frac{\hbar^2}{2m}\nabla^2\sqrt{\rho_1(\mathbf{r})}+[U_{\rm ext}(\mathbf{r})-\mu+V_{\rm SC}(\mathbf{r})]\sqrt{\rho_1(\mathbf{r})} \tag{4.2}$$

with

$$V_{\rm SC}(\mathbf{r}_1)=\frac{1}{2\sqrt{\rho_1(\mathbf{r}_1)}}\frac{\delta E_{(2)}}{\delta\sqrt{\rho_1(\mathbf{r}_1)}}=\frac{\delta E_{(2)}}{\delta\rho_1(\mathbf{r}_1)}=\int d^3r_2\,\rho_1(\mathbf{r}_2)g(\mathbf{r}_1,\mathbf{r}_2)v_{\rm JF}(\mathbf{r}_1,\mathbf{r}_2)$$
$$+\tfrac{1}{2}\int d^3r_2\,d^3r_3\,\rho_1(\mathbf{r}_2)\rho_1(\mathbf{r}_3)v_{\rm JF}(\mathbf{r}_2,\mathbf{r}_3)\frac{\delta g(\mathbf{r}_2,\mathbf{r}_3)}{\delta\rho_1(\mathbf{r}_1)}+\frac{\hbar^2}{8m\rho_1(\mathbf{r}_1)}\int d^3r_2\,\rho_1(\mathbf{r}_2)\nabla_1[g(\mathbf{r}_1,\mathbf{r}_2)\rho_1(\mathbf{r}_1)\nabla_1 u_2(\mathbf{r}_1,\mathbf{r}_2)]\ . \tag{4.3}$$

Note that Eq. (4.3) may be understood as the generalization of the Hartree equation for spatially correlated systems; it reduces to the ordinary Hartree equation if we set the two-body correlation function $u_2(\mathbf{r}_1,\mathbf{r}_2)$ to zero.

The only term appearing in Eq. (4.3) that requires further manipulations is the density derivative of the two-body distribution function. The easiest way to analyze this term is to recall the diagrammatic meaning of the variational derivative with respect to the one-body density, which leads to

$$\int d^3r_2\,d^2r_3\,\rho_1(\mathbf{r}_2)\rho_1(\mathbf{r}_3)\frac{\delta g(\mathbf{r}_2,\mathbf{r}_3)}{\delta\rho(\mathbf{r}_1)}v_{\rm JF}(\mathbf{r}_2,\mathbf{r}_3)$$
$$=\int d^3r_2\,d^3r_3\left[[g(\mathbf{r}_1,\mathbf{r}_2)-1][g(\mathbf{r}_1,\mathbf{r}_3)-1]X'(\mathbf{r}_2,\mathbf{r}_3)+\frac{\delta E(\mathbf{r}_2,\mathbf{r}_3)}{\delta\rho_1(\mathbf{r}_1)}g'(\mathbf{r}_2,\mathbf{r}_3)\right]\rho_1(\mathbf{r}_2)\rho_1(\mathbf{r}_3) \tag{4.4}$$

where $X'(\mathbf{r}_2,\mathbf{r}_3)$ and $g'(\mathbf{r}_2,\mathbf{r}_3)$ are the diagrammatic quantities introduced in Sec. III [cf. Eqs. (3.9) and (3.10)]. An alternative derivation, straightforward though somewhat tedious, may be performed by taking the variational derivative with respect to the one-body density directly on the HNC equations (2.10) and (2.11).

With Eqs. (4.2)—(4.4) we have arrived at a representation of the generalized Hartree potential $V_{\rm SC}(\mathbf{r})$ in a form which does not rely on specific assumptions (e.g., optimization) of the two-body correlations. For example, one may use Eqs. (4.2)—(4.4) to determine the one-body density if one chooses to use some parametrized form for the two-body correlation function. It is, so far, exact within the Jastrow *ansatz* (2.1), though one will usually omit the elementary diagrams in a numerical application.

Some additional simplifications are feasible if one neglects the elementary diagrams and assumes that the two-body correlations are optimized. The main point is that the quantity $X'(\mathbf{r}_1,\mathbf{r}_2)$ may be eliminated, using the Euler-Lagrange equations (3.12) and (3.13), in favor of derivatives of the two-body correlations. It is, however, worth pointing out that the manipulations to follow are legitimate *only if the two-body correlations are in fact optimized.* For Schiff-Verlet correlation functions in bulk ^{4}He, for example, the optimization condition (3.12) is violated typically by an amount comparable to each of the sides of Eq. (3.12). The representation (4.2)—(4.4) is in such a case preferable since it always has the correct relation to the bulk pressure.

The above-mentioned elimination of $X'(\mathbf{r}_2,\mathbf{r}_3)$ in Eq. (4.4), which eliminates the Jackson-Feenberg potential by the particle-hole interaction, and the repeated use of the chain equation (2.11), lead to our final representation of the self-consistent one-body potential

$$V_{\rm SC}(\mathbf{r}_1)=V^{(1)}_{\rm SC}(\mathbf{r}_1)+V^{(2)}_{\rm SC}(\mathbf{r}_1) \tag{4.5}$$

with

$$V^{(1)}_{\rm SC}(\mathbf{r}_1)=\int d^3r_2\rho_1(\mathbf{r}_2)\left[V_{p\text{-}h}(\mathbf{r}_1,\mathbf{r}_2)-\frac{\hbar^2}{8m}\{[g(\mathbf{r}_1,\mathbf{r}_2)-1][D(1)+D(2)]N(\mathbf{r}_1,\mathbf{r}_2)+N(\mathbf{r}_1,\mathbf{r}_2)D(2)X(\mathbf{r}_1,\mathbf{r}_2)\}\right] \tag{4.6}$$

and

$$V^{(2)}_{\rm SC}(\mathbf{r}_1)=-\frac{\hbar^2}{16m}D(1)\int d^3r_2\rho_1(\mathbf{r}_2)[g(\mathbf{r}_1,\mathbf{r}_2)-1]N(\mathbf{r}_1,\mathbf{r}_2)\ . \tag{4.7}$$

V. STATIC FORM FACTOR IN THE RPA

To conclude the formal parts of our analysis of the variational theory of inhomogeneous Bose systems we show that the static form factor obtained through the

fluctuation-dissipation theorem from the density-density response function is given by the Euler-Lagrange equation (3.12). We assume a linear-response function of the usual RPA form

$$\chi(\mathbf{r}_1,\mathbf{r}_2;\omega)=\chi^0(\mathbf{r}_1,\mathbf{r}_2;\omega)+\int d^3r_3 d^3r_4 \chi^0(\mathbf{r}_1,\mathbf{r}_3;\omega) \times V_{p\text{-}h}(\mathbf{r}_3,\mathbf{r}_4)\chi(\mathbf{r}_4,\mathbf{r}_2;\omega) , \quad (5.1)$$

where $\chi^0(\mathbf{r}_1,\mathbf{r}_2;\omega)$ is the linear-response function of a noninteracting system, which is described in terms of the eigenfunctions of a one-body Hamiltonian alone. We assume that the single-particle wave functions are determined by a Hartree equation

$$\left[-\frac{\hbar^2}{2m}\nabla^2+V_H(\mathbf{r})\right]\phi_i(\mathbf{r})=\epsilon_i\phi_i(\mathbf{r}) , \quad (5.2)$$

where $V_H(\mathbf{r})$ is a local (self-consistent) Hartree potential which may depend implicitly on the eigenfunctions $\phi_i(\mathbf{r})$ of the one-body equation (5.2). Since we need in the following only relative excitation energies $e_i\equiv\epsilon_i-\epsilon_0$, we eliminate the local Hartree potential $V_H(\mathbf{r})$ in favor of the lowest eigenstate of Eq. (5.2). We find

$$H(1)\phi_i(\mathbf{r})=\left[-\frac{\hbar^2}{2m}\frac{1}{\phi_0(\mathbf{r})}\nabla\phi_0^2(\mathbf{r})\cdot\nabla\frac{1}{\phi_0(\mathbf{r})}\right]\phi_i(\mathbf{r}) =e_i\phi_i(\mathbf{r}) . \quad (5.3)$$

It is convenient to work in a spectral representation in terms of the eigenfunctions of this one-body Hamiltonian

$$H(1)=\sum_i \phi_i(\mathbf{r})e_i\phi_i(\mathbf{r}') , \quad (5.4)$$

i.e., $\chi^0(\mathbf{r}_1,\mathbf{r}_2;\omega)$ has the representation

$$\chi^0(\mathbf{r}_1,\mathbf{r}_2;\omega)=\sum_i \frac{2e_i\phi_0(\mathbf{r}_1)\phi_i(\mathbf{r}_1)\phi_i(\mathbf{r}_2)\phi_0(\mathbf{r}_2)}{\hbar^2\omega^2-e_i^2} . \quad (5.5)$$

In the corresponding matrix form,

$$\chi_{ij}(\omega)\equiv\int d^3r\, d^3r' \frac{\phi_i(\mathbf{r})}{\phi_0(\mathbf{r})}\chi(\mathbf{r},\mathbf{r}';\omega)\frac{\phi_j(\mathbf{r}')}{\phi_0(\mathbf{r}')} , \quad (5.6)$$

$$\chi^0_{ij}(\omega)\equiv\int d^3r\, d^3r' \frac{\phi_i(\mathbf{r})}{\phi_0(\mathbf{r})}\chi^0(\mathbf{r},\mathbf{r}';\omega)\frac{\phi_j(\mathbf{r}')}{\phi_0(\mathbf{r}')} =\frac{2e_i\delta_{ij}}{\hbar^2\omega^2-e_i^2} , \quad (5.7)$$

and

$$V_{ij}\equiv\int d^3r\, d^3r' \phi_0(\mathbf{r})\phi_i(\mathbf{r})V_{p\text{-}h}(\mathbf{r},\mathbf{r}')\phi_j(\mathbf{r}')\phi_0(\mathbf{r}') , \quad (5.8)$$

we find

$$\sum_k [(\hbar^2\omega^2-e_i^2)\delta_{ik}-2e_iV_{ik}]\chi_{kj}(\omega)=2e_i\delta_{ij} \quad (5.9)$$

or

$$\frac{1}{\sqrt{e_i}}\chi_{ij}(\omega)\frac{1}{\sqrt{e_j}}=2[(\hbar^2\omega^2-e_i^2)\delta_{ij}-2\sqrt{e_i}V_{ij}\sqrt{e_j}]^{-1} . \quad (5.10)$$

The form (5.10) is suitable for performing the frequency integral:

$$\frac{1}{\sqrt{e_i}}\mathrm{Im}\left[\int_{-\infty}^{\infty}\frac{d(\hbar\omega)}{2\pi}\chi_{ij}(\omega)\right]\frac{1}{\sqrt{e_j}} =(e_i^2\delta_{ij}+2\sqrt{e_i}V_{ij}\sqrt{e_j})^{-1/2} . \quad (5.11)$$

The relation (5.11) is most easily shown by adopting a representation in which the matrix $(e_i^2\delta_{ij}+2\sqrt{e_i}V_{ij}\sqrt{e_j})$ is diagonal.

To make contact with the distribution functions introduced in Sec. II, we introduce the static form factor

$$S(\mathbf{r},\mathbf{r}')=\frac{1}{\phi_0(\mathbf{r})\phi_0(\mathbf{r}')}\mathrm{Im}\left[\int_{-\infty}^{\infty}\frac{d(\hbar\omega)}{2\pi}\chi(\mathbf{r},\mathbf{r}';\omega)\right] \quad (5.12)$$

and the corresponding matrix representation

$$S_{ij}\equiv\mathrm{Im}\left[\int_{-\infty}^{\infty}\frac{d(\hbar\omega)}{2\pi}\chi_{ij}(\omega)\right] . \quad (5.13)$$

To make the connection with the HNC equation (or, more precisely, to the chain equation) we define

$$S_{ij}=[(\underline{1}-\underline{X})^{-1}]_{ij} . \quad (5.14)$$

If we rewrite Eqs. (5.13) and (5.11) in terms of X_{ij}, we obtain finally

$$-X_{ik}e_k-e_iX_{ik}+\sum_j X_{ij}e_jX_{jk}=2V_{ik} , \quad (5.15)$$

which is the structural equivalent to the Euler-Lagrange equation (3.12). The final connection is made by identifying the lowest eigenstate of the one-body Hamiltonian $H(1)$ with the square root of the physical one-body density, i.e.,

$$H(1)=-\frac{\hbar^2}{2m}\frac{1}{\sqrt{\rho_1(\mathbf{r})}}\nabla\rho_1(\mathbf{r})\cdot\nabla\frac{1}{\sqrt{\rho_1(\mathbf{r})}} . \quad (5.16)$$

With this identification, Eqs. (5.15) and (3.12) are identical, and we have thereby completed the proof that the RPA is a proper subset of an optimized HNC. The HNC goes beyond the RPA in the sense that it provides an unambiguous prescription for the choice of the particle-hole interaction and the single-particle Hamiltonian.

VI. NUMERICAL OPTIMIZATION

The HNC equations (2.10) and (2.11), the two-body Euler-Lagrange equations (3.12) and (3.17), and the Hartree equation (4.2) with the self-consistent potentials (4.5)–(4.7) form a closed set of equations in the sense that they allow the determination of all quantities of interest from the bare two-body interaction $v(r)$, the external potential $U_{\mathrm{ext}}(\mathbf{r})$, and the number of particles in the system. For the sake of clarity, and to explain our iteration path, we repeat here the relations between the two-body functions $X(\mathbf{r}_1,\mathbf{r}_2)$, $N(\mathbf{r}_1,\mathbf{r}_2)$, and $g(\mathbf{r}_1,\mathbf{r}_2)$, and the Euler-Lagrange equation for these two-body quantities. The two-body Euler-Lagrange equation has been formulated for the set of "non-nodal" diagrams $X(\mathbf{r}_1,\mathbf{r}_2)$, which can be calculated from a given guess of the particle-hole in-

teraction $V_{p\text{-}h}(\mathbf{r}_1,\mathbf{r}_2)$:

$$\frac{\hbar^2}{4m}\{[D(1)+D(2)]X(\mathbf{r}_1,\mathbf{r}_2)-[X*DX](\mathbf{r}_1,\mathbf{r}_2)\} = V_{p\text{-}h}(\mathbf{r}_1,\mathbf{r}_2) . \quad (6.1)$$

We will see below that our algorithm of solving Eq. (6.1) gives us simultaneously the two-body distribution function $g(\mathbf{r}_1,\mathbf{r}_2)$, and hence the set of "nodal" diagrams $N(\mathbf{r}_1,\mathbf{r}_2)=g(\mathbf{r}_1,\mathbf{r}_2)-1-X(\mathbf{r}_1,\mathbf{r}_2)$. With this information, a next guess of the particle-hole interaction

$$V_{p\text{-}h}(\mathbf{r}_1,\mathbf{r}_3)=g(\mathbf{r}_1,\mathbf{r}_2)v(|\mathbf{r}_1-\mathbf{r}_2|)+\frac{\hbar^2}{2m}\{|\nabla_1[g(\mathbf{r}_1,\mathbf{r}_2)]^{1/2}|^2+|\nabla_2[g(\mathbf{r}_1,\mathbf{r}_2)]^{1/2}|^2\} + \frac{\hbar^2}{4m}[g(\mathbf{r}_1,\mathbf{r}_2)-1]\{[D(1)+D(2)]N(\mathbf{r}_1,\mathbf{r}_2)+[X*DX](\mathbf{r}_1,\mathbf{r}_2)\} \quad (6.2)$$

can be obtained. This formal statement is, of course, empty unless a prescription is given for how such an iteration path can be numerically verified. The amount of data to be handled depends essentially on the symmetries of the physical system under consideration. In a homogeneous liquid, all two-body quantities depend on only one coordinate, i.e., the distance between two particles. One needs typically 50 to 100 mesh points for a sufficiently accurate representation. In the next more complicated problem which allows for symmetry breaking in one direction (i.e., either a plane surface or a system with spherical symmetry), each two-body function depends nontrivially on three coordinates. Using the remaining symmetries and variable mesh sizes, we are still left with the problem of determining the function under consideration at about 10^5 points. An iterative procedure to determine such large numbers of data is clearly preferable to a linearization of the Euler-Lagrange equations as would be necessary in the representation of Ref. 10. Such a procedure would involve the inversion of a $10^5\times10^5$ matrix in each iteration, and one hesitates to undertake such an effort even if today it may be numerically feasible.

Let us specialize now to the special geometry that was used in our calculations. We consider a film of ^{4}He atoms which is translationally invariant in the x and y direction, and symmetric at $z=0$. In that geometry, all two-body quantities are functions of the z coordinates z_1,z_2 of each of the two particles, and their distance $r_{||}$ parallel to the surface. The quadratic term in $X(\mathbf{r},\mathbf{r}')$ is a convolution integral. Fourier transforming parallel to the surface decouples the equation for $X(z_1,z_2,q_{||})$ for each momentum $q_{||}$ parallel to the surface. We will see that the solution of this decoupled equation involves just the diagonalization of an $n\times n$ matrix, where n is the number of mesh points in the direction orthogonal to the surface.

Simultaneously with a new guess for the next approximation $X^{(n+1)}(\mathbf{r},\mathbf{r}')$, we obtain also a new guess for the two-body functions $g(\mathbf{r},\mathbf{r}')$ and $N(\mathbf{r},\mathbf{r}')$, and the associated changes

$$\delta X(\mathbf{r},\mathbf{r}')=X^{(n+1)}(\mathbf{r},\mathbf{r}')-X^{(n)}(\mathbf{r},\mathbf{r}') \quad (6.3)$$

and

$$\delta N(\mathbf{r},\mathbf{r}')=N^{(n+1)}(\mathbf{r},\mathbf{r}')-N^{(n)}(\mathbf{r},\mathbf{r}') . \quad (6.4)$$

However, the new pair-distribution function will not, during most of the iterations, have an acceptable behavior for small interparticle distances. The PPA uses therefore the nth approximation to the pair-distribution function $g^{(n)}(\mathbf{r},\mathbf{r}')$ as a damping factor, in other words the $(n+1)$st approximation for $g(\mathbf{r},\mathbf{r}')$ is taken to be

$$g^{(n+1)}(\mathbf{r},\mathbf{r}')=g^{(n)}(\mathbf{r},\mathbf{r}')\exp[\delta X(\mathbf{r},\mathbf{r}')+\delta N(\mathbf{r},\mathbf{r}')] . \quad (6.5)$$

[Note that the linearization of Eq. (2.10) yields $\delta u_2(\mathbf{r},\mathbf{r}')=\delta X(\mathbf{r},\mathbf{r}')$.] With these new guesses for the two-body quantities we calculate via Eq. (6.2) a new particle-hole interaction and repeat the procedure until convergence is reached.

The key to a solution of the optimization problem lies therefore in an efficient algorithm to solve the RPA equation (6.1). Our algorithm is intimately connected with the study of the normal modes of the system and will be described in detail in the next paper.[21] It suffices here to state that one must solve the eigenvalue problem

$$H^2(1)\psi^{(l)}(\mathbf{r})+2\int d^3r'\sqrt{\rho_1(\mathbf{r})}V_{p\text{-}h}(\mathbf{r},\mathbf{r}')\sqrt{\rho_1(\mathbf{r}')}H(1)\psi^{(l)}(\mathbf{r}')=\hbar^2\omega_l^2\psi^{(l)}(\mathbf{r}) . \quad (6.6)$$

It is then easily shown that the sum of non-nodal diagrams can be constructed via

$$X(\mathbf{r},\mathbf{r}')=\frac{1}{\sqrt{\rho_1(\mathbf{r})}}\left[\delta(\mathbf{r}-\mathbf{r}')-\sum_l\hbar\omega_l\psi^{(l)}(\mathbf{r})\psi^{(l)}(\mathbf{r}')\right]\frac{1}{\sqrt{\rho_1(\mathbf{r}')}} . \quad (6.7)$$

The pair-distribution function can be constructed in a similar manner:

$$g(\mathbf{r},\mathbf{r}')=1+\frac{1}{\sqrt{\rho_1(\mathbf{r})}}\left[\sum_l\frac{1}{\hbar\omega_l}[H(1)\psi^{(l)}(\mathbf{r})][H(1)\psi^{(l)}(\mathbf{r}')]-\delta(\mathbf{r}-\mathbf{r}')\right]\frac{1}{\sqrt{\rho_1(\mathbf{r}')}} . \quad (6.8)$$

We see that we can avoid the explicit solution of the chain equation (2.11) within the algorithm.

Compared with the solution of the two-body equation, the treatment of the one-body equation is quite easy. It helps to know that[21]

$$\frac{\delta V_{\rm SC}(\mathbf{r})}{\delta\rho_1(\mathbf{r}')} = V_{p\text{-}h}(\mathbf{r},\mathbf{r}') \ . \tag{6.9}$$

This form suggests that we write the one-body potential (4.5)—(4.7) as

$$V_{\rm SC}(\mathbf{r}) = \int d^3r'\, V_{p\text{-}h}(\mathbf{r},\mathbf{r}')\rho_1(\mathbf{r}') + \Delta V_{\rm SC}(\mathbf{r}) \ , \tag{6.10}$$

where the decomposition (6.10) is obvious from the structure of the one-body potential (4.5)—(4.7). For a given initial guess of the one-body density and the expressions (6.2) and (4.5)—(4.7) for that density, we solve the Hartree equation

$$0 = \left[-\frac{\hbar^2}{2m}\nabla^2 + \Delta V_{\rm SC}(\mathbf{r}) - \mu + \int d^3r'\, V_{p\text{-}h}(\mathbf{r},\mathbf{r}')\rho_1(\mathbf{r}') \right] \sqrt{\rho_1(\mathbf{r})} \ . \tag{6.11}$$

Equation (6.11) is readily solved by a Newton-Raphson procedure. It is advantageous to solve the one-body equation for a fixed particle number

$$n = \int_{-\infty}^{\infty} dz\, \rho_1(z) \ . \tag{6.12}$$

The chemical potential μ is considered as an additional unknown variable to be determined simultaneously with the solution of the Hartree equation.

The most difficult part of the numerical optimization is to find a suitable initial guess for the self-consistent Hartree potential. Using the solution of the optimization problem for bulk ^{4}He at the expected central density as a first guess and a density profile from, e.g., Ref. 11, leads generally to a repulsive single-particle potential which does not support a self-bound system. In order to obtain an attractive Hartree potential, we have to iterate the two-body equation a few times on the fixed background of an externally given density. After that, the density and the Hartree potential were updated after each iteration of the two-body equation. Having obtained a solution at a given particle number n, it takes six to ten iterations for a neighboring particle number to obtain an agreement between successive estimates of the densities and the total energy within three digits. The least stable quantity is the chemical potential μ which is therefore affected by the largest numerical uncertainty.

VII. APPLICATION TO FILMS OF ^{4}He

We have solved the optimization problem described in this paper for the above outlined geometry of films of free ^{4}He atoms which are translationally invariant in the x-y plane, and have a nontrivial spatial shape in the z direction. To judge the value of our results we recall that the HNC approximation for bulk ^{4}He yields values for the saturation energy and density, which are too low. The calculated equilibrium density of bulk ^{4}He, interacting via the Aziz potential,[22] is, in the HNC approximation, $\rho_0^{\rm HNC}=0.017$ Å^{-3}; the corresponding binding energy is -5.35 K. The equilibrium density falls short of the experimental value $\rho_0^{\rm expt}=0.0218$ Å^{-3} by about 30%. There is, of course, a great number of ways either to improve or to manipulate the calculation in order to obtain better agreement with experimental data. We have refrained in this paper from such manipulations in order to keep the computational effort small, and to keep the calculation as clean as possible.

A collection of our results for the ground-state energy, the chemical potential, and the central density for a set of different particle numbers per unit surface area is given in Table I. The central density and the chemical potential for the largest particle numbers agree well with the equilibrium properties found in bulk calculations.[23,24] Slight deviations are due to some sacrifices that were made in our calculation in order to keep the number of mesh points small. It appears that we have used a sufficiently large box which makes our results indistinguishable from the bulk limit in the center of the film.

The energies collected in Table I are to a good approximation a linear function of the particle number. We can therefore extract a surface energy σ using

$$2\sigma = E(n) - \mu_\infty n \ , \tag{7.1}$$

TABLE I. The energy per surface area (column 2), the total energy per particle (column 3), the chemical potential (column 4), and the central density of the film (column 5) are given for various particle numbers per surface area (column 1).

n (Å^{-2})	E/L^2 (K Å^{-2})	E/A (K)	μ (K)	ρ_c (Å^{-3})
0.13	−0.408	−3.14	−4.97	0.0140
0.14	−0.457	−3.26	−5.06	0.0145
0.15	−0.507	−3.38	−5.11	0.0149
0.16	−0.556	−3.48	−5.14	0.0154
0.18	−0.659	−3.66	−5.16	0.0158
0.20	−0.763	−3.82	−5.18	0.0162
0.22	−0.870	−3.95	−5.20	0.0165
0.24	−0.975	−4.06	−5.21	0.0167
0.26	−1.080	−4.15	−5.21	0.0168
0.28	−1.182	−4.22	−5.22	0.0170

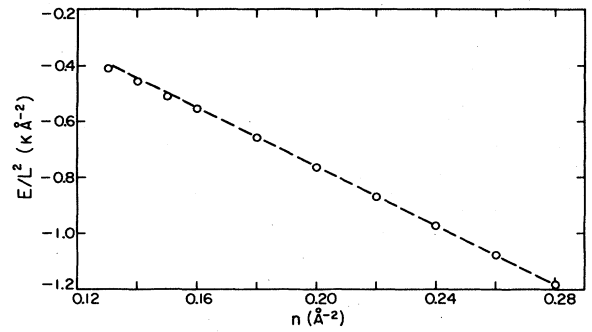

FIG. 1. Energy of the film per surface area E/L^2 is shown as a function of the number n of particles per surface area. The circles represent calculated values, and the dashed line shows the linear interpolation between films of the particle numbers $n=0.16$ Å^{-2} and $n=0.28$ Å^{-2}.

where μ_∞ is the asymptotic chemical potential. The energy per unit surface area in the particle-number range $n=0.16$ Å^{-2} and $n=0.28$ Å^{-2}, is, to good accuracy, a linear function of the particle number n per surface area (Fig. 1). A linear interpolation in that density regime leads to the values $\mu_\infty=-5.22$ K and $\sigma=0.14$ K Å^{-2}. The value of μ_∞ is consistent with the chemical potentials shown in Table I for the larger particle numbers. The surface energy σ falls short of the experimental values of $\sigma_{\text{expt}}=0.273$ K Å^{-2} by roughly a factor of 2. This difference is to be expected from the combined effect of the too low saturation energy and density in the HNC approximation. It should, of course, be recalled that we have performed a "no-parameter" calculation, the only experimental input being the microscopic two-body potential. There has been no fit whatsoever to properties of bulk ^{4}He.

Figure 2 shows the density profiles obtained in the present work for a variety of total particle numbers. The surface widths are comparable to those of Ref. 11; at the largest particle number we are in a regime where the system looks uniform in the middle of the film.

Figure 3 shows the pair-distribution function $g(\mathbf{r},\mathbf{r}')$ for two particles having the same distance z from the center of the film, as a function of their distance $r_\parallel$ parallel to the surface. The five curves show $g(\mathbf{r},\mathbf{r}')$ for the distances $z=1$, 3, 5, 7, and 9 Å from the center of the film, corresponding to 99%, 95%, 80%, 45%, and 7% of the central density. The distribution function at the lowest density shows the typical shape of a pair-distribution function in low density bulk ^{4}He, with the usual nearest-neighbor peak replaced by a broad maximum. Towards the center of the film, the solutions are close to the bulk $g(r)$ at the same density.

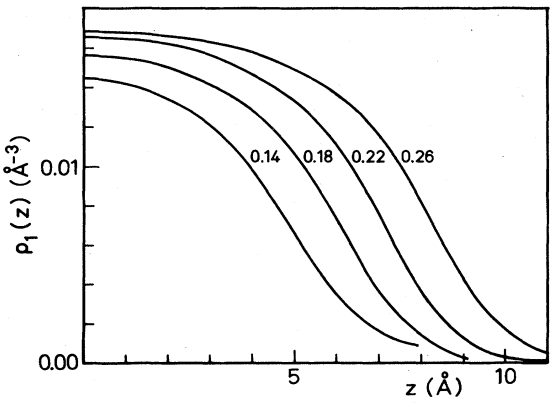

FIG. 2. Density profile of the ^{4}He films are shown for the particle numbers $n=0.14$, 0.18, 0.26 Å^{-2}. The density profile is symmetric at $z=0$.

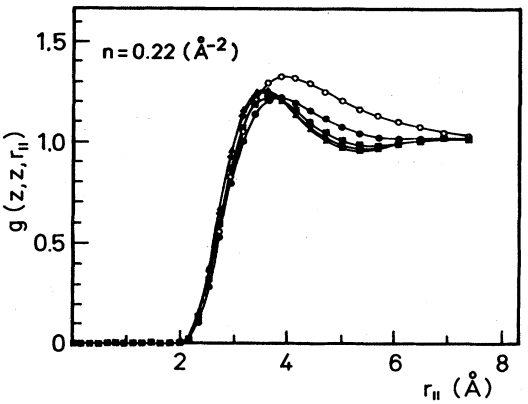

FIG. 3. Pair-distribution function $g(\mathbf{r},\mathbf{r}')$ is shown as a function of the distance $r_\parallel$ of the two particles *parallel* to the surface. Both particles have the same distance z from the center of the film. Open circles: $z=9$ Å; filled circles: $z=7$ Å; squares: $z=5$ Å; diamonds: $z=3$ Å; triangles: $z=1$ Å. The distribution function corresponds to the film with a particle number per unit area of $n=0.22$ Å^{-2}.

Figure 4 shows the pair-distribution function for two particles at zero distance parallel to the surface for the same values of the z coordinate of one of the particles as

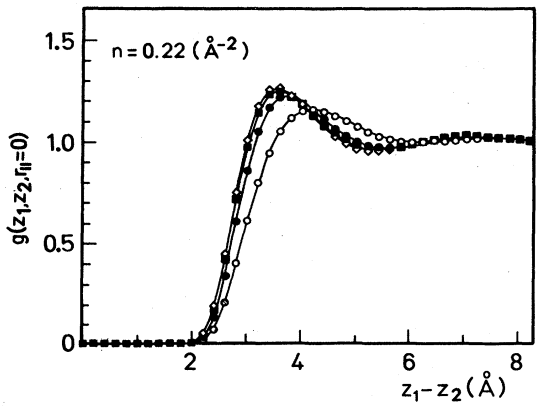

FIG. 4. Pair-distribution function $g(\mathbf{r},\mathbf{r}')$ is shown for two particles with $x=x', y=y'$. The first particle is located at distances $z_1=9$ Å (open circles), $z_1=7$ Å (filled circles), $z_1=5$ Å (squares), and $z_1=3$ Å (diamonds). The second particle is located at a distance z_1-z_2 to the left of the first one. The distribution functions for $z_1=1$ Å and $z_1=3$ Å are indistinguishable. The distribution functions correspond to the film with a particle number per unit area of $n=0.22$ Å^{-2}.

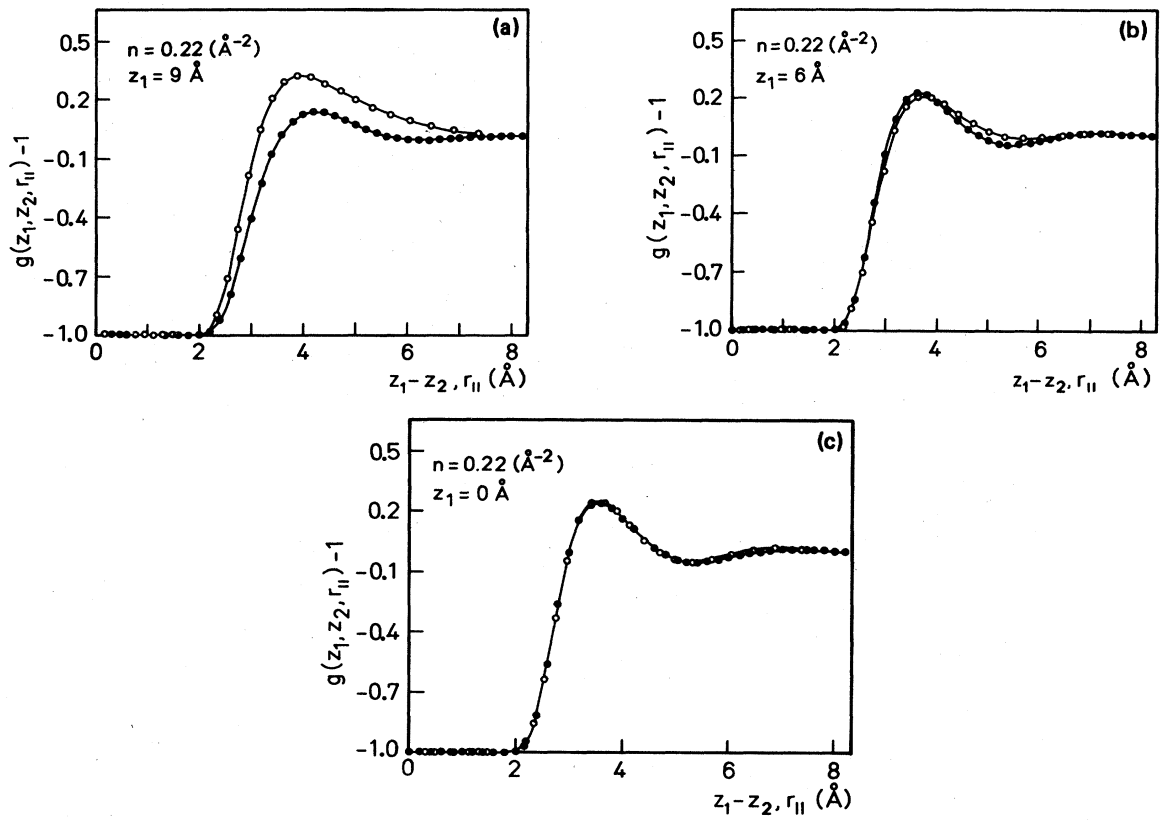

FIG. 5. (a) Pair-distribution function is shown for a particle located at a distance $z_1 = 9$ Å from the center of the film, in the direction parallel to the surface (open circles), and orthogonal to the surface to the left (filled circles). The distribution functions correspond to the film with a particle number per unit area of $n = 0.22$ Å^{-2}. (b) Same as (a) for $z_1 = 6$ Å. (c) Same as (a) for $z_1 = 0$.

used above. The second particle is located in the direction towards the center of the film. We find essentially the same picture as above. However, the nearest-neighbor peak of the distribution function for the reference particle located at the lowest density is weaker and shifted somewhat further away from the origin.

In view of frequency applied "local-density approximations," it is also of interest to study the anisotropy of the two-body distribution function. This is done in Figs. 5(a)—5(c) for a particle located at a distance of 9 and 6 Å away from the center of the film, and a particle located in the center. The corresponding densities are 7%, 66%, and 100% of the central density. The distribution function is shown in the direction parallel and perpendicular (inward) to the surface. We find a substantial degree of anisotropy only at the lowest density. From this one might be led to the conclusion that local-density approximations are essentially acceptable simplifications of the problem. The reader is, however, reminded of the fact that there are no solutions of the bulk HNC/EL equations below roughly 60% of the calculated saturation density. This behavior reflects the physical instability of a low-density fluid against droplet formation.[6]

VIII. SUMMARY

We have in this paper developed systematically the theory of correlations in a Bose liquid. To some extent it was necessary to review earlier derivations, in particular those of Saarela *et al.*,[10] in order to bring them into a form suitable for further manipulations and investigations.

Our formal derivations have produced the expected results: It is possible to formulate Euler-Lagrange equations to compute optimal correlations in an inhomogeneous system. The equations appear to be generalizations of the known representation of the Euler-Lagrange equations for homogeneous Bose fluids: The Feenberg representations (3.6), to which we devoted most of our work, is particularly suited to study the intermediate- and long-ranged correlations. It leads naturally to the paired-phonon analysis[17] as the appropriate optimization route.

What is at least as important as the formal developments is that we have designed a systematic scheme which can be implemented numerically. In brief, it is the understanding of the physical processes described by the distinct compound-diagrammatical quantities of HNC theory which leads to the development of an efficient optimization route.

Besides the numerical application of our method, important new formal developments are to be anticipated. The most prominent thrust of theoretical development goes toward the generalization of our theory to excited states[21] and to Fermi systems. The implementation of Fermi statistics seems to be possible with modest formal and numerical effort,[25] which should lead to a quantita-

tive theory of the surface of metals and liquid ^{3}He. The prospect of generalizing the theory to nuclear many-body systems is somewhat less promising, since the hypernetted-chain problem has not yet been solved for state-dependent correlations. Nevertheless, one might expect to derive from a generalization of the present, state-independent theory to simple Fermi systems a qualitative, microscopic understanding of nuclear shell-model potentials.

We have also shown in this paper that the numerical solution of the coupled HNC-EL equations is a very practical approach: As soon as one decides to work with anisotropic correlations the amount of data to be handled is comparable for optimized and nonoptimized calculations. One iteration of the PPA equations is about a factor of 5 or 6 more time consuming than one iteration of the HNC equations. The PPA iterations converge in fact faster than the iterative determination of the one-body potential, hence no advantage is gained by keeping a fixed pair correlation during these iterations. We conclude therefore that an optimized HNC treatment of an inhomogeneous system is at most a factor of 5—10 more time consuming than a single HNC calculation with a fixed pair-correlation function. This estimate does not yet account for possible parameter searches to minimize the energy in a nonoptimized HNC calculation. We regard therefore the assumption of isotropic pair-correlation functions as an unnecessary oversimplification.

We have restricted ourselves here to the demonstration of the general route by which optimized HNC calculations for inhomogeneous systems can be efficiently performed. A few numerical sacrifices were made in order to decrease the computational effort. In that sense, our work is comparable to the pioneering work of Campbell and Feenberg,[17] who in their development of the PPA first designed a general and efficient algorithm for the optimization of the pair correlations in bulk Bose liquids. This work was ultimately led to the high-precision calculations and stability studies of Castillejo *et al.*[6] We anticipate a similar development for the inhomogeneous case.

In the field of physical interest we anticipate a broad array of application on thin films and their collective modes. The case of a free surface is the most demanding since there is no force to keep the particles in place. Imposition of an external field over the particles should only help the convergence. The next immediate goal is the extension of the present theory to collective states which we pursue, in a slightly simplified model, in the next paper[21] of this series.

Note added in proof. After this paper was finished we became aware of some related work by Piper *et al.*,[26] who included, in a variational Monte Carlo calculation of droplets of ^{4}He, the three-body factor $u_3(\mathbf{r}_i,\mathbf{r}_j,\mathbf{r}_k)$ in the Feenberg function. None of the correlation factors was optimized by an Euler-Lagrangian equation, and the two-body correlations were assumed to be spherically symmetric. Consequently, these authors arrive at a weaker anisotropy of the pair-distribution function $g(\mathbf{r}_1,\mathbf{r}_2)$. We refer to the above discussion of Figs. 5(a)—5(c) for very general physical arguments that the stronger anisotropy found in our work is the expected behavior.

ACKNOWLEDGMENTS

We would like to thank R. A. Smith for providing us with very accurate solutions of the bulk ^{4}He problem. This research was supported in part by the Deutsche Forschungsgemeinschaft (E.K.), by National Science Foundation Grants Nos. DMR-81-14556 and PHY-77-27084, supplemented by funds from the U.S. National Aeronautics and Space Administration, as well as by the U.S. Office of Naval Research Contract No. N00014-82-K-0626.

*Present address: Department of Physics, Texas A&M University, College Station, TX 77843.

[1]D. M. Ceperley and B. J. Adler, Phys. Rev. Lett. **45**, 566 (1980).
[2]M. H. Kalos, M. A. Lee, P. A. Whitlock, and G. V. Chester, Phys. Rev. B **24**, 115 (1981).
[3]M. A. Lee, K. E. Schmidt, M. H. Kalos, and G. V. Chester, Phys. Rev. Lett. **46**, 728 (1981).
[4]E. Feenberg, *Theory of Quantum Fluids* (Academic, New York, 1969).
[5]A. D. Jackson, A. Lande, and R. A. Smith, Phys. Rep. **86**, 55 (1982).
[6]L. Castillejo, A. D, Jackson, B. K. Jennings, and R. A. Smith, Phys. Rev. B **20**, 3631 (1979).
[7]E. Krotscheck, in *Quantum Fluids and Solids, Sanibel, Florida, 1983,* Proceedings of the Symposium on Quantum Fluids and Solids, edited by E. D. Adams and G. G. Ihas (AIP, New York, 1983).
[8]Y. M. Shih and C.-W. Woo, Phys. Rev. Lett. **30**, 478 (1973); F. D. Mackie and C.-W. Woo, Phys. Rev. B **18**, 529 (1978).
[9]C. C. Chang and M. Cohen, Phys. Rev. A **8**, 1930 (1973).
[10]M. Saarela, P. Pietiläinen, and A. Kallio, Phys. Rev. B **27**, 231 (1983).
[11]V. R. Pandharipande, J. G. Zabolitzky, S. C. Pieper, R. B. Wiringa, and U. Helmbrecht, Phys. Rev. Lett. **50**, 1676 (1983).
[12]E. Krotscheck, Phys. Rev. A **15**, 397 (1977).
[13]T. Morita and K. Hiroike, Prog. Theor. Phys. **25**, 537 (1961).
[14]T. Morita, Prog. Theor. Phys. **20**, 920 (1958).
[15]J. G. Zabolitzky (private communication).
[16]N. Iwamoto, E. Krotscheck, and D. Pines, Phys. Rev. B **29**, 3936 (1984).
[17]C. E. Campbell and E. Feenberg, Phys. Rev. **188**, 396 (1969).
[18]L. J. Lantto and P. J. Siemens, Phys. Lett. **68B**, 308 (1977).
[19]A. D. Jackson, L. J. Lantto, and P. J. Siemens, Phys. Lett. **68B**, 311 (1977).
[20]E. Krotscheck, Phys. Rev. A **26**, 3536 (1982).
[21]E. Krotscheck, following paper, Phys. Rev. B **31**, 4258 (1985).
[22]R. A. Aziz, V. P. S. Nain, J. C. Carley, W. L. Taylor, and G. T. McConville, J. Chem. Phys. **70**, 4330 (1979).
[23]L. R. Whitney, F. J. Pinski, and C. E. Campbell, J. Low Temp. Phys. **44**, 367 (1981).
[24]R. A. Smith (private communication).
[25]E. Krotscheck , Phys. Rev. B (to be published).
[26]S. C. Piper, R. B. Wiringa, and V. R. Pandharipande, (unpublished).